Water Adsorption on Environmental Metal Oxides and Atmospheric Dusts Determined by the Diffuse Reflectance Infrared Fourier Transform Spectroscopy (DRIFTS) Technique

Shane McDemos, Rachel Sechan, Alden Walkley, Tobin Thorton, Declan Bates, Christopher W. Harmon

Introduction:

Environmental metal oxides (EMO) have multiple chemical and physical interactions with the environment.[1] Dust storms and agriculture are the main contributors to introducing EMO from the surface to the atmosphere as seen in **Figure 1.**[2] The composition of the Earth's surface crust is dispersed with various metal oxides as seen in **Table 1.**[3]

TABLE 1: Abundance of Major Elements and associated oxides in the Upper Continental Crust (from Ref. 3)

Element	% Abundance	Oxide	% Abundance
Si	30.348	SiO_2	61.5
Al	7.744	Al_2O_3	15.1
Fe	3.089	Fe_2O_3	6.28
Ca	2.945	CaO	5.5
K	2.865	K_2O	2.4
Na	2.567	Na_2O	3.2
Mg	1.351	MgO	3.7
Ti	0.3117	TiO_2	0.68
Ba	0.0668	BaO	0.0584
Mn	0.0527	MnO	0.1

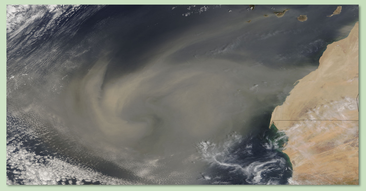

Figure 1: Dust storm from the coast of West Africa and the Sahara Desert taken Sept. 2012.[2]

Particulate matter (PM) plays an important role in cloud formation because it acts as a nuclei for water vapor, leading to the formation of cloud droplets. The solid/air interface serves as the initial site where water molecules begin to aggregate and form molecular, or mono-, layers and eventually tiny liquid droplets on the surface of these dust particles, which is dependent on atmospheric conditions.

EMOs are an abundant component of atmospheric dust, PM, and minerals, and provide surfaces onto which water vapor can adhere and accumulate. As the ambient relative humidity (RH) rises, water vapor comes into contact with these PMs, forming a thin layer of water quantified by the number of monolayers (Θ_w). This process continues as more water vapor condenses onto the existing monolayers, gradually building up and forming larger droplets. These initial stages of cloud formation, facilitated by PM, are essential for the subsequent growth and development of clouds. As more water vapor condenses and accumulates around these nuclei, the cloud droplets grow in size until they become visible clouds. Therefore, understanding the properties and behavior of EMOs in the atmosphere and their behavior in PM is crucial for comprehending the processes underlying cloud formation and precipitation.

Methodology

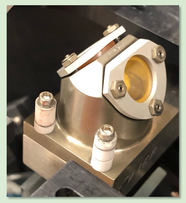

Figure 2: DRIFTS (Diffuse Reflectance Infrared Fourier Transform Spectroscopy) apparatus and gas manifold. DRIFTS technique is a form of infrared spectroscopy specialized in analyzing the IR spectra of solid (powder) surfaces. The DRIFTS cell apparatus is placed inside an FTIR that produces and analyzes infrared frequencies that reflect through the DRIFTS cell and sample after absorption. Mass flow controllers (MFC) are capable of gas flow outputs at variable flow rates to introduce both dry ultra-high purity (UHP) N_2 and humid UHP N_2 to the DRIFTS cell. A calibrated Vaisala RH Probe (HMT 130) quantifies the % RH before entering the DRIFTS cell, which is carefully temperature-controlled to maintain a steady and reliable RH.

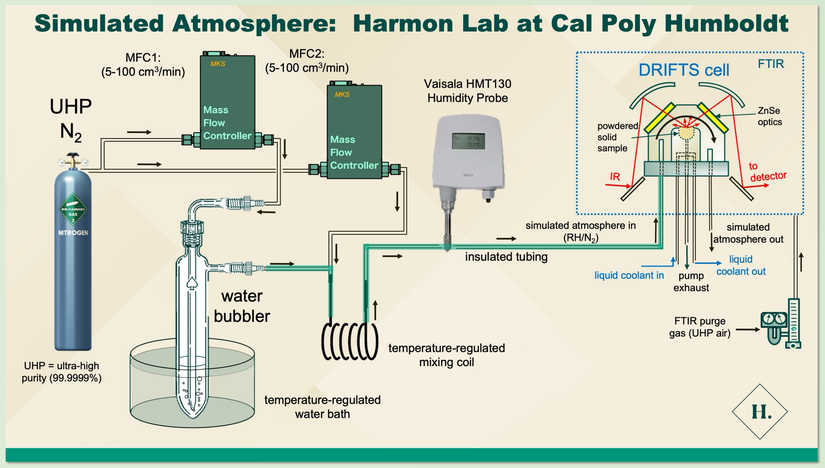

Results and Discussion

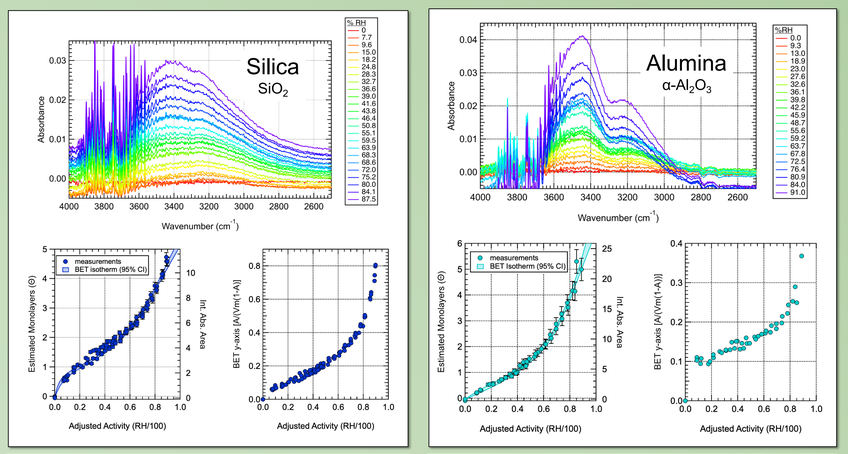

Figure 3: DRIFTS spectra of adsorbed water (top), integrated area, and estimated number of water monolayers (bottom left), and BET plot (bottom right) of various samples investigated.

***TABLE 2: Arizona Test Dust Composition**

Component	% Abundance
SiO_2	69–77
Al_2O_3	8–14
CaO	2.5–5
K_2O	2–5
Na_2O	1–4
Fe_2O_3	4–7
MgO	1–2
TiO_2	0–1

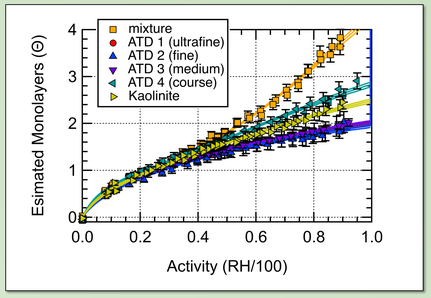

Figure 4: A comparison of silica dominate particles, all of which behave very similar at low % RH

B.E.T. Adsorption Isotherms

$$V \propto \int_{\tilde{\nu}_i}^{\tilde{\nu}_f} A d\tilde{\nu} \quad (1) \qquad A_w = \frac{P}{P_o} = \frac{RH}{100} \quad (2)$$

$$C = \exp\left(\frac{\Delta H_1 - \Delta H_2}{RT}\right) \quad (3)$$

$$\Theta_w = \frac{V}{V_m} = \frac{CA_w}{(1-A_w)(1-A_w+CA_w)} \quad (4)$$

$$\frac{A_w}{V(1-A_w)} = \frac{1}{CV_m} + \left(\frac{(C-1)}{CV_m}\right) A_w \quad (5)$$

$$y = b + m\,x$$

Equation 1 demonstrates the initial assumption in that the integrated absorbance spectrum (***A***) is proportional to the volume (***V***) of an adsorbed water layer, which is confirmed by literature.[4–6] Water Activity (***Aw***) is defined by equation 2 as ratio of the vapor pressure of water (***P***) to its saturation vapor pressure (***Po***), or % relative humidity (**RH**) divided by 100. Equation 3 defines the B.E.T. constant, ***C***, where $\Delta H_{2/1}$ are the enthalpy of vaporization of the bulk (2) and first layer (1) of water, respectively. Equation 4 is the *classic* B.E.T. equation, where ***Vm*** is the volume of water required to make one monolayer, ***Θw*** is the number of water monolayers, and ***V***, ***C***, and ***Aw*** have been defined above.[7]

Equation 5 is the linear form of the B.E.T. equation, where the slope (***m***) and intercept (***b***) are related to the ***C*** and ***Vm*** constants shown above.[7] This form of the equation is only linear between 0 and ~35% RH and is used to determine B.E.T. parameters.[7] Equation 6 is a modified version of the B.E.T. equation that assumes the surface will become saturated by a maximum number of adsorbate layers (***n***) at saturation vapor pressures, whereas equation 4 assumes there will be an infinite number.[7] Previous studies have determined equation 6 is more appropriate for EMO than equation 4.[4] Equation 7 is a similar rearrangement of equation 6 as was done with equations 4 and 5. The same slope (***m***) and intercept (***b***) are determined in equation 7 compared to equation 5 over the linear range (0–35%RH), and we propose the use of a power term (Kx^n), or perhaps something similar, to approximate the higher-order terms. Thus, B.E.T. plots will be generated with ***Aw/V(1-Aw)*** as the y-axis, allowing us to determine ***Vm***, ***C***, and ***n*** as well as ***Θw*** as a function of ***Aw*** and confirming the B.E.T. isotherm is adequateate for describing the water uptake of EMO.

$$\Theta_w = \frac{V}{V_m} = \left(\frac{CA_w}{1-A_w}\right)\left(\frac{1-(n+1){A_w}^n + n{A_w}^{n+1}}{1+(C-1)A_w - C{A_w}^{n+1}}\right) \quad (6)$$

$$\frac{A_w}{V(1-A_w)} = \frac{1}{CV_m} + \left(\frac{(C-1)}{CV_m}\right)A_w - \frac{{A_w}^{n+1}}{V_m} + \frac{A_w}{V(1-A_w)}\left(n{A_w}^{n+1} + {A_w}^{n+1} - n{A_w}^{n+2}\right)$$

$$y = b + m\,x + K\,x^n \quad (7)$$

Table 3: Results of B.E.T Analysis

(d_p)	SiO_2	α-Al_2O_3	α-Fe_2O_3	Mixture	ATD 1 (4.85 µm)	ATD 2 (16.73 µm)	ATD 3 (25.19 µm)	ATD 4 (47.78 µm)	Kaolinite
C	20.07 ± 4.66	3.201 ± 0.930	6.195 ± 0.956	11.84 ± 1.60	10.72 ± 0.71	8.904 ± 1.020	10.13 ± 0.53	12.44 ± 1.61	10.25 ± 0.98
n	9.585 ± 0.569	13.49 ± 1.53	6.814 ± 0.73	7.652 ± 0.162	3.099 ± 0.047	3.052 ± 0.084	3.219 ± 0.034	4.772 ± 0.107	4.089 ± 0.087
V_m	2.377 ± 0.076	4.314 ± 0.373	4.833 ± 0.392	1.844 ± 0.0737	33.79 ± 4.37	14.53 ± 1.07	19.59 ± 1.40	13.93 ± 0.81	14.07 ± 1.58

Table 3 shows a summary of the results. As can be seen, particles that are silica dominate have very similar ***C*** constant values, ranging between 8–12. The mixture was made to be similar to that of Arizona Test Dust (ATD), shown in Table 2. Different sizes (d_p = average particle diameter) of ATD are available and standardized. Interestingly, the different sizes have very similar behavior in the low % RH (indicative of a similar ***C*** constant) but very different behavior at high % RH. This will be explored in future research.

References

(1.) Chen, L.; Peng, C.; Gu, W.; Fu, H.; Jian, X.; Zhang, H.; Zhang, G.; Zhu, J.; Wang, X.; Tang, M. On mineral dust aerosol hygroscopicity. *Atmospheric Chemistry and Physics* **2020**, *20* (21), 13611–13626.

(2.) Ichoku, C. NASA/Goddard Spaceflight Center, 2007. http://visibleearth.nasa.gov/.

(3.) Wedepohl, K. H., The composition of the continental crust. *Geochim. Cosmochim. Acta* **1995,** *59* (7), 1217–1232.

(4.) Ma, Q.; He, H.; Liu, Y. In situ drifts study of hygroscopic behavior of mineral aerosol. *Journal of Environmental Sciences* **2010**, *22* (4), 555–560.

(5.) Hatch, C. D.; Wiese, J. S.; Crane, C. C.; Harris, K. J.; Kloss, H. G.; Baltrusaitis, J. Water adsorption on clay minerals as a function of relative humidity: Application of BET and freundlich adsorption models. *Langmuir* **2012**, *28* (3), 1790–1803.

(6.) Al-Abadleh, H. A.; Grassian, V. H. FT-IR study of water adsorption on aluminum oxide surfaces. *Langmuir* **2002**, *19* (2), 341–347.

(7.) Brunauer, S.; Deming, L. S.; Deming, W. E.; Teller, E. On a theory of the van der waals adsorption of gases. *Journal of the American Chemical Society* **1940**, *62* (7), 1723–1732.